Overall and Local Bread Expansion, Mechanical Properties, and Molecular Structure During Bread Baking: Effect of Emulsifying Starches

Milica Pojić, Maja Musse, Corinne C. Rondeau-Mouro, M. Hadnadev, François Mariette, M. Cambert, Y. Diascorn, S. Quellec, A. Torbica, T.D. Hadnadev, et al.

Overall and Local Bread Expansion, Mechanical Properties, and Molecular Structure During Bread Baking: Effect of Emulsifying Starches

Milica Pojić, Maja Musse, Corinne Rondeau, Miroslav Hadnađev, David Grenier, François Mariette, Mireille Cambert, Yves Diascorn, et al.

Food and Bioprocess Technology
An International Journal

ISSN 1935-5130

Food Bioprocess Technol
DOI 10.1007/s11947-016-1713-2

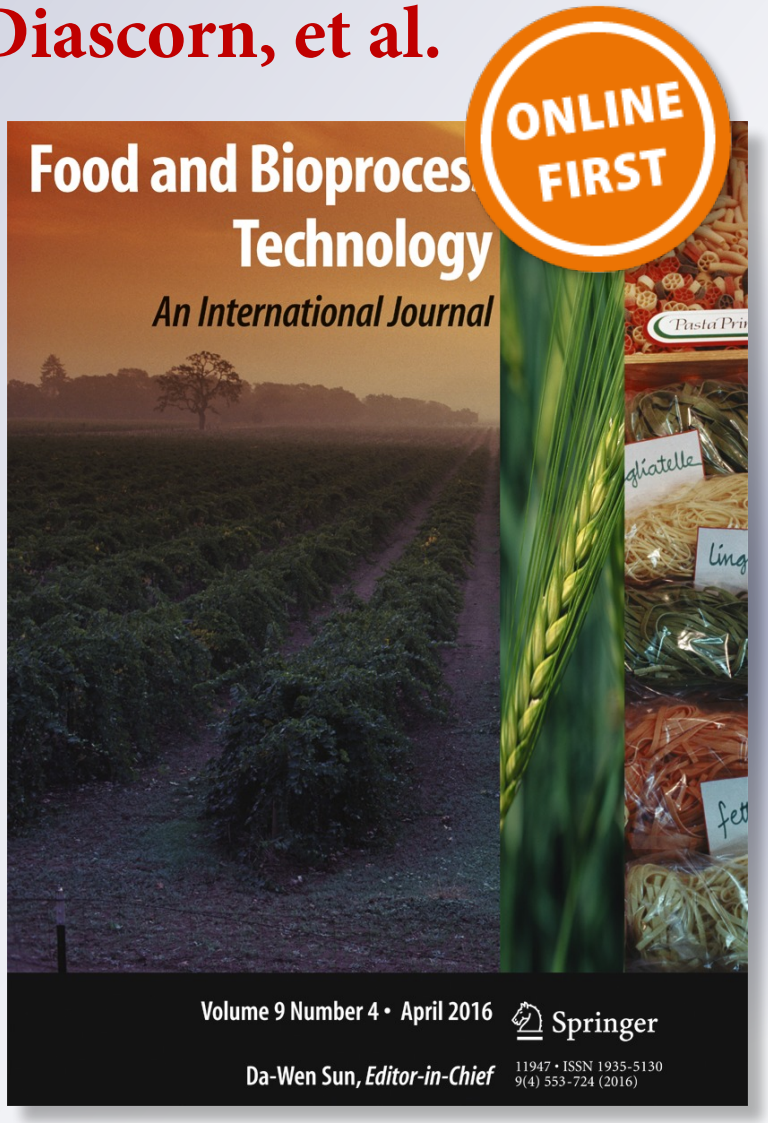

Springer

Food Bioprocess Technol
DOI 10.1007/s11947-016-1713-2

ORIGINAL PAPER

Overall and Local Bread Expansion, Mechanical Properties, and Molecular Structure During Bread Baking: Effect of Emulsifying Starches

Milica Pojić[1] · Maja Musse[2] · Corinne Rondeau[2] · Miroslav Hadnađev[1] · David Grenier[2] · François Mariette[2] · Mireille Cambert[2] · Yves Diascorn[2] · Stéphane Quellec[2] · Aleksandra Torbica[1] · Tamara Dapčević Hadnađev[1] · Tiphaine Lucas[2]

Received: 9 November 2015 / Accepted: 1 March 2016

Abstract In order to determine the relationship between molecular structure of wheat bread dough, its mechanical properties, total and local bread expansion during baking and final bread quality, different methods (rheological, nuclear magnetic resonance, magnetic resonance imaging and general bread characterisation) were employed. The study was extended on wheat dough with starch modified by octenyl succinic anhydride (OSA) in order to generalise the results. The interest of investigating multi-scale changes occurring in dough at different phases of baking process by considering overall results was demonstrated. It was found that OSA starch improved the baking performance during the first phase of baking. This feature was due to a higher absorption of water by OSA starch granules occurring at temperatures below that of starch gelatinization, as confirmed by NMR, and consecutive higher resistance to deformation for OSA dough in this temperature range (20–60 °C). This was explained by a delayed collapse of cell walls in the bottom of the OSA dough. In the second phase of baking (60–80 °C), the mechanism of shrinkage reduced the volume gained by OSA dough during the first phase of baking due to higher rigidity of OSA dough and its higher resistance to deformation. MRI monitoring of the inflation during baking made it possible to distinguish the qualities and defaults coming from the addition of OSA starch as well as to suggest the possible mechanisms at the origin of such dough behaviour.

Keywords Nuclear magnetic resonance (NMR) · Magnetic resonance imaging (MRI) · Transverse relaxation time (T2) · OSA starch · Oven rise · Creep recovery test

Introduction

Bread dough made of flour, water and yeast is a multicomponent, multi-scale product (Aguilera 2005; Lakes 1993). It consists of starch-gluten matrix in which many bubbles develop (from about 10 % in gas fraction at the end of mixing up to about 70 % at the end of fermentation), with diameters ranged from a few tenths of μm at the end of mixing to a few millimeters at the end of baking. The starch-gluten matrix forms walls between bubbles with thickness representing a couple of hundreds of microns or lower, according to reports at the end of proving or baking (Besbes et al. 2013; Turbin-Orger et al. 2012). The mechanical properties of dough walls partly determine the potential of bubbles to properly inflate without rupturing all along the bread-making process. During baking, the more or less progressive cessation of inflation due to increasing dough resistance of rupturing is deeply controlled by the evolving molecular structure of dough walls. Interactions and hydration of macromolecules (gluten and starch components) locally evolve according to their own hydrothermal trajectory. The heterogeneous hydrothermal treatment imposed by baking, within a convective or deck oven, generates heterogeneities in hydrothermal local trajectories which, in turn, lead to

✉ Maja Musse
maja.musse@irstea.fr

[1] Institute of Food Technology, University of Novi Sad, Bulevar cara Lazara 1, 21000 Novi Sad, Serbia

[2] Irstea, UR OPAALE, 17 Avenue de Cucillé-CS 64427, F-35044 Rennes cedex, France

Published online: 19 March 2016

spatial heterogeneities in bubble and wall sizes, state of macromolecules (protein coagulation and starch gelatinisation) and gas formation (Mondal and Datta 2008; Lucas et al. 2008). These deep heterogeneous changes in the molecular structure and gas generation during baking make it one of the most critical steps over the bread-making process in mastering the final bread structure.

Molecular mechanisms involved in controlling the water transport at microscopic scale and mechanical behaviour of the dough can be approached using proton time domain nuclear magnetic resonance (TD-NMR) as demonstrated for a wide range of dough products (e.g. Bosmans et al. 2012, 2013b; Curti et al. 2011, 2014; Doona and Baik 2007). In dough, the use of TD-NMR aimed at investigating the evolution of the biopolymer structure (mainly starch and gluten) between unbaked and baked, yet cooled samples (Bosmans et al. 2012; Doona and Baik 2007; Engelsen et al. 2001; Wang et al. 2004) or stored bread samples, in relation to starch retrogradation (Bosmans et al. 2013a; Chen et al. 1997; Curti et al. 2011; Wynnejones and Blanshard 1986). Very recently, NMR measurements have been performed during bread baking, showing that the changes with temperature of each NMR signal component (T2 value and the associated relative intensity) allowed to monitor separately the starch reversible swelling and gelatinization processes (Rondeau-Mouro et al. 2015).

In addition to molecular changes, dough, as an evolving viscoelastic and shear thinning material, undergoes different types and magnitudes of deformation during the bread-making process (Mirsaeedghazi et al. 2008). Mixing is associated with extreme deformations which are lowered during the first fermentation stage. Sheeting and molding are associated with deformations of an intermediate magnitude. Finally, during baking, deformations are low compared with those of preceding steps (Dobraszczyk and Morgenstern 2003), but occur at an already high deformation level of the bubble walls, that can hardly be considered within the small strain domain (strain > 0.1 m/m). Rheological studies on dough related to baking have been generally performed using small deformation, shear oscillation tests at room temperature (Dobraszczyk and Morgenstern 2003). So far, none of the reports have shown the creep and recovery response of dough measured under a gradual increase in temperature corresponding to that of bread baking. Disposal of such data could doubtlessly be helpful in feeding baking and mechanical model of viscoelasticity using fitting and parameter identification methods (Kim et al. 2008; Laridon et al. 2015).

At last, inflation of bubbles was successfully monitored by tomographic techniques like X-rays or magnetic resonance imaging (MRI). The measurements are dynamic and non-invasive, a crucial feature for fragile dough. Previous studies showed how far the mechanical constrains like those generated at the shaping step (Van Duynhoven et al. 2003; Whitworth and Alava 2004) or at the baking step by the crust setting (Wagner et al. 2008a; Bajd and Sersa 2011) can generate heterogeneities in gas fraction through the dough section and competition for expansion between dough regions.

Different phenomena occurring during bread-baking were mostly studied independently using specific methodologies. The links between data obtained from these studies are therefore hard to establish, particularly as differences in samples used (i.e. flour functionality) may introduce important consequences on the results (Gil 2003). Therefore, in order to gain a comprehensive interpretation of the dough behaviour observed at macroscopic level, it should be coupled with phenomena observed at the microscopic and mesoscopic level (Schiraldi and Fessas 2003).

The first objective of the present paper was to characterize multi-scale changes in dough during baking, to attempt to relate the different scales between each other as well as to the final bread properties (volume, texture and colour). The molecular level was characterised by NMR during bread baking and its impact on the mechanical properties of the dough (determined by creep and recovery tests) was also assessed dynamically during heating. At about the same scale as rheological measurements, even larger (centimetric scale), MRI was used to monitor changes occurring in the local gaseous phase. Finally, the overall dough volume was also monitored by MRI. Furthermore, a common bread formulation was slightly modified by incorporation of starch modified with octenyl succinic anhydride (OSA starch). This approach made it possible to generalise the conclusions of the present study with different bread formulations.

The second objective to this paper was to evaluate if OSA starch can act as a bread improver, by investigating its effects on mechanical properties and overall loaf expansion. Indeed, OSA starches so far have been used to stabilize flavour emulsion in beverages (Reiner et al. 2010), oil in salad dressings, to encapsulate flavour, as emulsifier in sauces, puddings and baby foods (Dokić et al. 2012) and as fat replacers in muffins (Chung et al. 2010). However, the reports on their application in bread making so far is limited (Hadnađev et al. 2014).

Materials and Methods

Materials

Wheat flour (13.61 ± 0.25 % moisture, 73.14 ± 1.08 % starch, 23.7 ± 1.68 % wet gluten, 9.24 ± 0.43 % protein, 1.72 ± 0.06 % total sugar, 0.97 ± 0.09 % fat, 0.90 ± 0.03 % total dietary fibre, 0.42 ± 0.05 % ash) and native gluten (8.14 ± 0.15 % moisture, 80.56 ± 1.63 % protein, 2 g/g water binding capacity) were provided from Fidelinka milling company, Serbia. The commercial quality of wheat flour was described by a Farinograph water absorption of 52.3 %, a softening degree of 65 BU, an

Alveograph deformation energy of $144 \cdot 10^{-4}$J and an Amylograph peak viscosity of 1230 BU. The sodium octenyl succinate starch (OSA starch encoded C*EmTex 06328) (15.02 ± 0.27 % moisture) was obtained from waxy maize starch and provided from Cargill, France. The control dough formulation (hereinafter referred as CONTROL) used for rheological, NMR and MRI measurements was comprised of wheat flour and water, while OSA dough formulation (hereinafter referred as OSA) was comprised of wheat flour in which 10 % (*w*/*w*) was replaced by OSA starch and native gluten flour in the same proportion as in the control flour. Both formulations were prepared at fixed dough water content of 44.7 % to provide the reliable interpretation of NMR results.

Bread (CONTROL and OSA) was prepared with fresh brewer yeast (2.5 % of flour weight). The dough for bread samples intended for subsequent measurements was mixed in a l-shaped mixer for 17 min (Diosna, Germany) and then fermented in mass at ambient temperature (19 ± 2 °C); volume was multiplied by 2.2, within about 45 min. After first proving, the dough was divided into pieces (390 g for final product characterization and 180 g for MRI baking experiment), rounded, rested for 15 min and shaped into loaves, which were placed in two types of the pans depending on the measurement to be performed: teflon pans (Tefal, France) (L × W × H: 240 × 85 × 65 mm) for final product characterization and glass-made pans covered with teflon for MRI baking experiment (L × W × H: 190 × 70 × 70 mm). The final dough proving was performed in a cabinet (35 °C, 85 % RH) until the initial volume was multiplied by 2.8 (about 55 min). The increases in dough volume were checked with a graduated proving tester (25 g). Samples for NMR measurements were taken from such prepared dough. Bread for final product characterization was baked at 220 °C for 23 min in two tier oven (Termotehnika, Croatia). Subsequently, loaves were removed from the pans and allowed to cool for 2 h.

MRI baking experiment was performed in a specific oven compatible with MRI. Wagner et al. (2008b) showed that the characteristics (specific volumes, water loss, time course changes in temperature, crust coloration) of bread loaves baked in such MRI compatible oven were within the range of values reported in the literature for convection oven.

Methods

Rheological Measurements

The dough for creep and recovery measurements was prepared in a Mixolab mixing bowl (Chopin Technologies, France) using the following settings: mixing speed 80 rpm, mixing temperature 30 °C, mixing time 8 min and fixed water absorption to obtain dough with water content of 44.7 %. This water content was set for optimal consistency of CONTROL dough. After kneading, the obtained dough sample was rested for 10 min in a closed plastic bag at 20 °C in order to prevent water evaporation and to allow residual stresses to relax.

Creep and recovery measurements were carried out using a Haake Mars rheometer in a shearing mode (Thermo Scientific, Germany) equipped with PP35 S serrated parallel plate measuring geometry (35-mm diameter, 2-mm gap) in order to prevent dough slippage. After loading, the excess dough at the plate edges was neatly trimmed and the edges sealed with paraffin oil to prevent the dough from drying during measurements. Measurements were performed at ten different temperatures in the range of 20–90 ± 0.1 °C (20, 30, 40, 50, 60, 65, 73, 76, 80 and 90 °C) applied onto the same dough piece. These temperatures were measured into the dough sample. After each change in temperature set, a 15-min waiting period was applied before testing in order to reach the next temperature point and, at the same time, to relax the sample from residual stresses. Creep was recorded at a shear stress of 70 Pa for 150 s, followed by a recovery phase of 450 s at a stress of 0 Pa (which was enough for reaching a plateau). The parameters obtained were: maximum creep compliance (J_{max}), zero shear viscosity (η_0), recovery value (J_e/J_{max}) which indicated the relative elastic part of J_{max} and relative viscous part of J_{max} (J_v/J_{max}). All rheological measurements were performed in triplicate.

NMR Measurements

^{1}H NMR measurements were performed using a Time-Domain spectrometer (Minispec Bruker, Germany) operating at a resonance frequency of 20 MHz. The NMR system was equipped with a temperature control device connected to a calibrated optical fiber (Neoptix Inc., Canada) allowing ±0.1 °C temperature regulation. The spin–spin relaxation (T2) was measured using the free induction decay (FID) and Carr-Purcell-Meiboom-Gill (CPMG) pulse sequences. The sampling rate for the acquisition of the FID was one point per 0.4 μs, and the delay between the 90° and 180° pulses of the CPMG sequence was 0.1 ms. Eight scans were recorded with a recycle delay of 2 s. The measurements were performed by step of 10 °C between 20 and 90 °C, by waiting an equilibrium temperature of 15 min before the signal acquisition. A final measurement was recorded after cooling the sample at 20 °C (after a waiting time of 15 min). The NMR tube preparation (in triplicate or quadruplicate) and the signal fitting were performed using the methods developed in (Rondeau-Mouro et al. 2015).

MRI and Temperature Measurements

MRI evaluation of local expansion in bread crumb during baking was performed using the method based on the incorporation of oil microcapsules into dough before dough shaping (Wagner et al. 2008a). The differences in the MRI signal

between microcapsules and dough enhanced by using the appropriate imaging sequence enabled the monitoring of the position of a microcapsule throughout the baking process. Dough was prepared as described in "Materials", but at the shaping step, a dough piece (180 g) was stretched into an 8-mm-thick band to allow the incorporation of microcapsule strips which were placed on the surface of dough band before rolling it manually. The lateral internal faces and bottom of the MRI compatible glass mould were coated with microcapsules before putting the dough into it. Additional strips were deposited onto the top surface of the dough. The dough was then submitted to the second proving step as described in "Materials".

Just before baking, four optical fibers (Ø 1 mm), connected to a data logger (model 790, Luxtron, USA), were inserted into the dough from a lateral side, in the length direction, at mid-length, of the dough, and used to measure temperature during the MRI baking experiment. The temperature gradient was characterized along a vertical line from the bottom crust to the top crust (few millimetres from the corresponding surfaces) at mid-width; the other two positions were in crumb near the crust and in the core crumb (two positions at about 30 and 40 mm from the bottom).

Bread loaves were baked in a convection oven installed within the probe of the MRI imager (see (Wagner et al. 2008b) for a detailed description of this oven). A 1.5T MRI scanner (Magnetom, Avanto, Siemens, Germany) equipped with a head receiver coil was used for measurements. Images of dough cross-section were acquired using a Fast Spin Echo (FSE) sequence with acceleration factor 3, acquisition matrix 128 × 70, field of view 128 × 70 mm^2, slice thickness 5 mm, echo time (TE) 7 ms, repetition time (TR) 200 ms, 3 excitations and acquisition time 15 s. Imaging sequence was launched in queue, making it possible to monitor dough during a 30-min baking period. At the end of baking, the coordinates (x, y) of the head of optical fibers were measured at the end of baking, after slicing the bread loaf. The experiment was repeated twice for each sample.

Image processing was performed using ImageJ software (National Institutes of Health, USA). Each microcapsule was first identified automatically on MRI images using thresholding method based on the entropy of the histogram algorithm (Kapur et al. 1985); its position corresponds to the barycentre of the bright spot composed of several pixels. Triangular elementary regions for calculating porosity were then defined manually between three neighbouring tracers. The surface of each triangle was deduced from the three coordinates. Finally, regions of similar behaviour towards expansion were pooled and considered together for analysis of local expansion. Global dimensions (height and width) as well as total area of the dough section as delimited by the microcapsule strips deposited on the dough surfaces were also calculated.

Last, relative changes in surface relative to its value at the onset of baking, S_r, were calculated:

$$S_{rd}(t) = \frac{S_d(t) - S_d(0)}{S_d(0)} \quad (1)$$

$$S_{ri}(t) = \frac{S_i(t) - S_i(0)}{S_i(0)} \quad (2)$$

where d refers to the total cross-section of dough in MRI images, and i denotes a region of the dough section (either a specific triangle delimited by three microcaspsules cross-section, or a group of these triangles), of which total number I covers the total cross section of dough. The relation between Eqs. 1 and 2 is:

$$S_{rd}(t) = \sum_{i=0}^{I} \omega_i S_{ri}(t) \quad (3)$$

with ω_i, the proportion occupied by the region i in the total dough section at the onset of baking

$$\omega_i = \frac{S_i(0)}{S_d(0)} \quad (4)$$

$\omega_i S_{ri}(t)$ in Eq. 3 is a contribution of the region i to relative changes in total surface at a given baking time t.

Bread Characterisation

Volume The specific volume of the bread loaves was determined by measuring the volume of millet seeds displaced by the weighed sample two hours after baking and cooling to ambient temperature (Cauvain and Young 2009). Specific volume was calculated as volume/weight (cm^3/g) of four loaves. The moisture of the breadcrumb was determined according to ICC 110/1 (ICC 1996) 2 hours after baking in triplicates.

Crumb Texture Crumb texture was assessed by performing a texture profile analysis (TPA) using a Texture Analyser (TA-XT2*i*, Stable Micro Systems, UK) equipped with a 30-kg load cell and a 75-mm diameter aluminium compression platen. The measurements were performed on crumb pieces (45-mm diameter and 12.5-mm thickness) taken from the central slices of the each loaf 2 h after baking. The selected settings included: 1 mm/s pre-test speed, 5 mm/s test and post-test speed and 80 % compression. The breadcrumb samples were compressed twice to give a two bite texture profile curve, with resting time of 5 s between two compression cycles (Bourne 2002). The recorded parameters were hardness, cohesiveness, springiness, chewiness and resilience. The TPA analysis was performed in five replicates.

Crust and Crumb Colors The colour of bread (crumb and crust) was measured by the Minolta Chroma Meter (CR-400) colorimeter (Konica Minolta Sensing Inc., Japan) equipped with standard illuminant D65. The colorimeter was calibrated before measurement with white standard tiles ($Y=93.7$, $X=0.3158$, $y=0.3324$). The results were recorded according to the CIELab colour, where the determined parameters were expressed as L^* describing lightness ($L^*=0$ for black, $L^*=100$ for white), a^* describing intensity in green-red ($a^*<0$ for green, $a^*>0$ for red), b^* describing intensity in blue-yellow ($b^*<0$ for blue, $b^*>0$ for yellow. Whiteness index (WI), total colour difference (ΔE) and browning index (BI) were calculated using obtained L^*, a^* and b^* values to describe the colour change as compared to control sample, as follows (Saricoban and Yilmaz 2010):

$$WI = 100-\sqrt{\left(100-L^*\right)^2 + a^{*2} + b^{*2}} \tag{5}$$

$$\Delta E = \sqrt{\left(L_0-L^*\right)^2 + \left(a_0-a^*\right)^2 + \left(b_0-b^*\right)^2} \tag{6}$$

$$BI = \frac{[100 \times (x-0.31)]}{0.17} \tag{7}$$

where:

$$x = \frac{\left(a^* + 1.75 \times L^*\right)}{\left(5.645 \times L^* + a^* - 3.012 \times b^*\right)} \tag{8}$$

If $\Delta E<1$, the colour differences are not considered obvious for the human eye; $1<\Delta E<3$, the colour differences are not considered appreciated for the human eye; $\Delta E>3$; the colour differences are considered obvious for the human eye (Francis and Clydesdale 1975). The crumb colour was measured in five, while the crust colour was measured in 15 replicates per loaf on the central slices two hours after baking.

Shrinkage of Dough Slabs Under Drying

Dough was laminated down to 2 to 3 mm approximately and four slabs of external dimensions 15 × 15 cm were cut off this dough sheet. Dough sticking during sheeting and further handling was avoided using microcrystalline cellulose, which presents the advantage to low affinity to water compared to flour. Dough slabs were returned, placed upside down onto a tray, pierced with a fork to avoid bubble growth and allowed to relax for 10 min before being placed into a deck oven (MIWE, Germany) for drying. The oven was preheated at 140 °C, and the set temperature was increased to 220 °C at the placement of dough slabs in the oven, and then decreased to 200 °C 3 min after the placement of dough slabs; following such procedure, time-temperature changes in the dough slabs were close to those measured in the top crust of a genuine bread loaf during baking.

At different time intervals, dough slabs were taken out of the oven. Their mass was measured, and a picture of their top surfaces was taken. The tray on which the dough slabs lied was placed back into the oven. The whole interruption did not last more than 1 min. Water content and water loss from dough slabs were estimated from the mass. The pictures were segmented using Image J, and the surface of dough slabs was estimated by counting the number of pixels belonging to the mask obtained from thresholding.

The whole experiment was repeated more than 7 times for each dough system.

Unidirectional shrinkage was then estimated from these surfaces, as follows

$$\text{shrinkage} = 1-\sqrt{\frac{s^{\text{dough}}(t)}{s^{\text{dough}}(0)}} \tag{10}$$

where $s^{\text{dough}}(t)$ is the top surface of the four dough slabs at time t.

Statistical Data Analysis

A one-way analysis of variance (ANOVA) was used to test the significant differences of the results of NMR and rheological measurements, each obtained at different temperatures, as well as of the results of bread characterization, for two bread formulations (CONTROL and OSA). ANOVA was followed by Fisher's least significant difference test, where the differences between means at the 5 % level ($p<0.05$) were considered significant. Statistical analysis was performed using Statgraphics XVI.I (Centurion) for NMR measurements and Statistica 10.0 (Statsoft, USA) for rheological and bread formulation measurements.

Results

Results are presented and discussed gradually from the molecular scale to the loaf scale, from the baking process to the final product once cooled down. With this ordering of presentation, cross discussion between results is managed in a natural manner as new results are presented. For each scale or technique of measurement, features common to both dough systems (OSA and CONTROL) are presented and discussed first, while differences between recipes are focused on in a separate section.

Changes at the Molecular Scale

Temperature-Associated Changes

T2 relaxation times have been measured under the same conditions for CONTROL and OSA dough upon heating. Five T2 components could be measured at 20 °C (Table 1), two of them from the FID signal and three from the CPMG one.

Based on previous work on model systems (Rondeau-Mouro et al. 2015), the component (1) around 19 μs represented non-exchangeable CH protons mainly from amylopectin crystallites and also from more or less structured amylose. The component (2) relaxing at 50–60 μs was characteristic of non-exchangeable protons of amorphous starch (mainly amylose) and from gluten chains with few contacts with water. Water in exchange with labile protons (OH−, NH−, SH−) from starch (mainly, water in granules) and gluten gave the third component (3) with a short T2 value around 2 ms, while water in exchange with gluten in the outside of sheets and with amylose and pentosans in extra-granule spaces of granules is more mobile and was then assigned to the fourth component (4) which relaxed at 9–10 ms. Additionally, to these four components found in starch-based model systems, dough was characterized by a fifth signal component with T2 around 25 ms (5), supposed to represent a second fraction of extra-granule water in slow diffusional exchange with the water layer at the surface of granules and of gluten sheets (Rondeau-Mouro et al. 2015).

By heating the samples above the ambient, variations in the T2 distributions suggested some proton transfers between the various proton populations, so between components (2) and (1) (Fig. 1a), but also between the FID (components (1) and (2)) and CPMG signals (water fractions (3), (4) and (5)), (Fig. 1b, Table 2). During the reversible swelling process with focus here between 20 and 50 °C, the decrease in the relative intensity of component (1) could not be explained only by the Curie's law (linear dependence of the magnetic susceptibility against the inverse of temperature). This phenomenon already explained by Rondeau-Mouro et al. (2015) lies on a proton transfer characteristics of an amylose loss from component (1) towards the amorphous zones of granules, component (2), and the extra-granular water phase, component (4) the latter showing an increase in its relative intensity as shown in Fig. 1b (dotted lines). These proton exchanges are well illustrated by a significant variation in I(1) in favor of I(2) and I(4) (Table 2). This leaching process can occur at ambient temperature when starch granules reversibly swell (Jenkins and Donald 1998), and it explains why we measured so short T2 relaxation times for the more mobile water fraction in products. Likewise, the reversible swelling process was clearly demonstrated by the net decrease in the relative intensity of component (5) with heating at low temperatures, concurrent with the rise of the relative intensity of component (2) typical of the enrichment

Table 1 T2 values (in ms) and relative intensity (in %) measured on the total NMR signal at 20 °C before (bh) and after (ah) heating

	T2(1)	I(1)	T2(2)	I(2)	I(1)+I(2)	T2(3)	I(3)	T2(4)	I(4)	T2(5)	I(5)	I(3)+I(4)+I(5)
CONT bh	0.0186 ± 0.0007^{1}	30.0 ± 0.3^{3}	0.0576 ± 0.0104^{1}	5.9 ± 0.8^{1}	35.9 ± 0.6	2.0 ± 0.2^{1}	14.5 ± 0.9^{1}	9.7 ± 0.9^{1}	25.0 ± 3.6^{1}	25.4 ± 2.1^{1}	24.6 ± 4.6^{1}	64.1 ± 3.0
OSA bh	$0.0189 \pm 0.0003^{1,2}$	29.8 ± 0.6^{3}	0.0606 ± 0.0036^{1}	5.7 ± 0.8^{1}	35.6 ± 0.7	2.0 ± 0.3^{1}	15.2 ± 1.6^{1}	9.8 ± 1.2^{1}	26.4 ± 1.6^{1}	24.8 ± 1.7^{1}	22.9 ± 3.5^{1}	64.4 ± 6.2
CONT ah	0.0239 ± 0.0066^{2}	17.4 ± 1.8^{2}	0.1274 ± 0.0717^{2}	16.7 ± 2.1^{2}	34.0 ± 2.0	4.0 ± 1.4^{2}	25.6 ± 8.1^{2}	12.4 ± 1.9^{2}	38.8 ± 8.7^{2}	130.4 ± 59.6^{2}	1.6 ± 1.5^{3}	66.0 ± 6.1
OSA ah	0.01780 ± 0.0016^{1}	9.9 ± 3.5^{1}	0.0578 ± 0.0082^{1}	19.5 ± 2.6^{2}	29.4 ± 3.1	1.3 ± 0.7^{1}	13.6 ± 2.0^{1}	9.2 ± 0.6^{1}	47.4 ± 10.4^{2}	35.9 ± 9.8^{2}	9.6 ± 6.5^{2}	70.6 ± 6.3

Mean value ± standard deviation. Values followed by the same number in the column are not significantly different ($p > 0.05$)

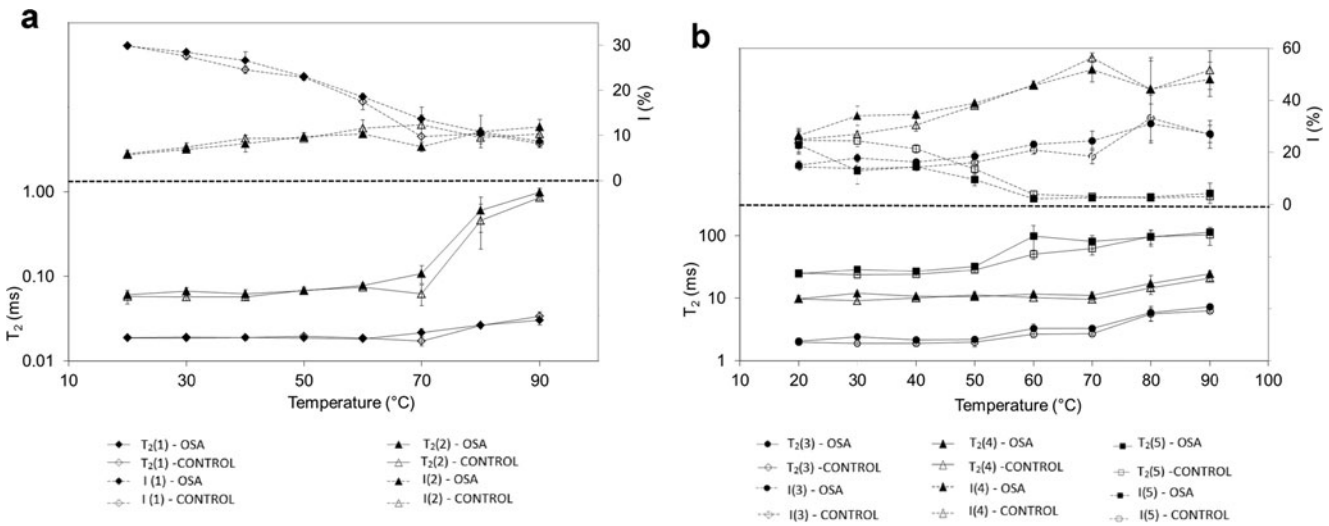

Fig. 1 T2 values in logarithmic scale and relative intensity measured as a function of temperature in CONTROL and OSA doughs from the **a** FID and **b** CPMG signals

of protons in the amorphous regions of starch granules. The values of T2 showed no significant differences and remained relatively constant between 20 and 50 °C for all components because of compensating mechanisms such as water sorption and amylose leaching (Rondeau-Mouro et al. 2015).

By increasing the temperature to 60 °C and up to 90 °C, the gelatinization of starch granules occurred; it contributed to the starch loss in crystallinity and organization, resulting in starch solubilization (mainly the amylopectin fraction) and disintegration of the granule (Donald 2004). Consistently, the relative intensity of component (1) (Fig. 1a) seemed to decrease in favor of the water fractions (3), (4) and (5) (Fig. 1b). Because of this, transfers of water protons in this temperature range were hardly noticeable from T2 values. A net increase in the T2 values was noticed and underlined by statistical tests (Table 2), above 70 °C for all T2 components but particularly for component (2) (Fig. 1a). This phenomenon already observed by (Rondeau-Mouro et al. 2015) and could be linked to thermal activation mechanisms (accordingly to Arrhenius' law). The reason why the T2 value increased was more pronounced for component (2), was related to the starch disintegration but also to the gluten denaturation, a process during which the protons of the water expelled from gluten and starch and polymer fractions should be characterized by a higher mobility (Bosmans et al. 2012).

About the Differences Between OSA and Control

At 20 °C before heating, equivalent T2 values ($p > 0.05$) and relative intensities were observed (Table 1). At higher temperatures (30–40 °C) but below the temperature commonly accepted for the onset of starch gelatinisation (60 °C), some significant differences between OSA and CONTROL doughs were observed for the T2 components (3) to (5) assigned to water protons in exchange (Fig. 1b, Table 2). Indeed, the OSA sample displayed a significantly lower relative intensity for component (5) compared to that of the CONTROL sample, for the benefit of the relative intensity of the component (4) and to a lesser extent that of the component (3), assigned to water protons in closer interactions with starch granules and its constituents. These results confirmed that OSA-starch favours the reversible water sorption above 20 °C.

Between 60 and 90 °C, significant differences in relative intensity were observed for components (1) and (2) (Fig. 1a, Table 2), in accordance with a higher proportion and longer chains of amylopectins in OSA dough. The use of OSA-starch in dough should extend the gelatinization process over to higher temperatures. Indeed, higher gelatinization temperature was observed by DSC for OSA starch (69.7 instead of 63.1 °C for CONTROL flour). It has already been shown that the branch lengths in B-type double helices of starches such as potato starch are larger than for A-type starches and should confer a better stability against heating (Waigh et al. 2000). These results showed a high sensitivity of NMR to this delayed gelatinisation. Moreover, the T2 values of component (2) tended to be shorter in CONTROL dough, especially at 70 °C. This evolution in T2 values was already discussed by Rondeau-Mouro et al (2015) who highlighted a significant T2(2) decrease for salted dough compared to unsalted dough. It was supposed to arise from weaker inter-macromolecule interactions compared to salted dough characterized by higher ionic interaction between sodium cations and macromolecules (Chiotelli et al. 2002; Rondeau-Mouro et al. 2015). The same explanation can also be used to compare CONTROL to OSA doughs; this last showing higher amylose and/or gluten mobility supposed to originate from weaker inter- and/or intra-macromolecular interactions may be due to the higher water sorption capacity of OSA starch.

Table 2 Changes in T2 values and relative intensities of CONTROL and OSA dough during heating; all data from this Table are reported in Fig. 1. Mean and standard deviation of 3–4 runs

		20 °C	30 °C	40 °C	50 °C	60 °C	70 °C	80 °C	90 °C
T2(1)	**CONTROL**	$0.0186 \pm 0.0007^{a,1}$	$0.0187 \pm 0.0012^{a,1}$	$0.0190 \pm 0.0011^{a,1}$	$0.0195 \pm 0.0005^{a,1}$	$0.0188 \pm 0.0006^{a,1}$	$0.0173 \pm 0.0021^{a,1}$	$0.0262 \pm 0.0017^{b,1}$	$0.0338 \pm 0.0043^{c,1}$
	OSA	$0.0189 \pm 0.0003^{a,1}$	$0.0191 \pm 0.0010^{ab,1}$	$0.0190 \pm 0.0014^{a,1}$	$0.0187 \pm 0.0009^{a,1}$	$0.0183 \pm 0.0002^{a,1}$	$0.0217 \pm 0.0024^{b,1}$	$0.0265 \pm 0.0004^{c,1}$	$0.0303 \pm 0.0039^{d,1}$
I(1)	**CONTROL**	$30.0 \pm 0.3^{e,1}$	$27.6 \pm 0.7^{d,1}$	$24.6 \pm 0.7^{c,1}$	$22.9 \pm 0.7^{c,1}$	$17.5 \pm 1.8^{b,1}$	$9.7 \pm 3.1^{a,1}$	$10.4 \pm 1.3^{a,1}$	$8.1 \pm 0.8^{a,1}$
	OSA	$29.8 \pm 0.6^{g,1}$	$28.5 \pm 0.6^{g,1}$	$26.6 \pm 1.9^{f,1}$	$23.1 \pm 0.5^{e,1}$	$18.5 \pm 0.5^{d,1}$	$13.7 \pm 0.8^{c,1}$	$10.8 \pm 0.8^{b,1}$	$8.7 \pm 1.0^{a,1}$
T2(2)	**CONTROL**	$0.0576 \pm 0.0104^{a,1}$	$0.0574 \pm 0.0054^{a,1}$	$0.0569 \pm 0.0045^{a,1}$	$0.0685 \pm 0.0054^{a,1}$	$0.0746 \pm 0.0038^{a,1}$	$0.0622 \pm 0.0171^{a,1}$	$0.4622 \pm 0.2505^{b,1}$	$0.8549 \pm 0.0476^{c,1}$
	OSA	$0.0606 \pm 0.0.0036^{a,1}$	$0.0663 \pm 0.0069^{a,1}$	$0.0619 \pm 0.0070^{a,1}$	$0.0672 \pm 0.0039^{a,1}$	$0.0776 \pm 0.0056^{a,1}$	$0.1077 \pm 0.0263^{a,2}$	$0.6024 \pm 0.2706^{b,1}$	$0.9942 \pm 0.1143^{c,1}$
I(2)	**CONTROL**	$5.9 \pm 0.8^{a,1}$	$7.4 \pm 1.0^{ab,1}$	$9.3 \pm 0.7^{bc,1}$	$9.4 \pm 0.7^{bc,1}$	$11.6 \pm 1.9^{cd,1}$	$12.4 \pm 3.9^{d,1}$	$9.5 \pm 1.4^{bc,1}$	$10.3 \pm 1.7^{cd,1}$
	OSA	$5.7 \pm 0.3^{a,1}$	$6.9 \pm 0.7^{ab,1}$	$8.1 \pm 1.9^{bcd,1}$	$9.7 \pm 0.9^{cde,1}$	$10.3 \pm 0.5^{de,1}$	$7.4 \pm 1.1^{abc,1}$	$10.8 \pm 3.5^{e,1}$	$11.8 \pm 1.7^{e,1}$
T2(3)	**CONTROL**	$2.0 \pm 0.2^{ab,1}$	$1.9 \pm 0.1^{a,1}$	$1.9 \pm 0.1^{a,1}$	$2.0 \pm 0.3^{ab,1}$	$2.7 \pm 0.3^{b,1}$	$2.7 \pm 0.2^{b,1}$	$5.6 \pm 1.3^{c,1}$	$6.3 \pm 0.4^{c,1}$
	OSA	$2.0 \pm 0.3^{ab,1}$	$2.4 \pm 0.2^{ab,2}$	$2.1 \pm 0.2^{a,1}$	$2.2 \pm 0.2^{ab,1}$	$3.3 \pm 0.6^{b,1}$	$3.3 \pm 0.3^{b,1}$	$5.8 \pm 1.5^{c,1}$	$7.3 \pm 0.3^{c,2}$
I(3)	**CONTROL**	$14.5 \pm 0.9^{a,1}$	$13.7 \pm 0.8^{a,1}$	$14.3 \pm 0.5^{a,1}$	$16.2 \pm 1.8^{ab,1}$	$20.8 \pm 1.6^{b,1}$	$18.4 \pm 2.9^{ab,1}$	$33.2 \pm 8.8^{d,1}$	$26.9 \pm 5.4^{c,1}$
	OSA	$15.1 \pm 1.6^{a,1}$	$17.8 \pm 1.6^{a,2}$	$16.3 \pm 0.6^{a,2}$	$18.6 \pm 1.8^{ab,1}$	$23.1 \pm 1.2^{bc,1}$	$24.4 \pm 3.8^{c,1}$	$31.1 \pm 7.5^{d,1}$	$27.1 \pm 3.3^{cd,1}$
T2(4)	**CONTROL**	$9.7 \pm 0.9^{ab,1}$	$9.2 \pm 0.3^{a,1}$	$10.0 \pm 0.8^{ab,1}$	$11.3 \pm 1.1^{b,1}$	$10.3 \pm 0.3^{ab,1}$	$9.5 \pm 0.6^{a,1}$	$14.7 \pm 1.7^{c,1}$	$21.0 \pm 2.4^{d,1}$
	OSA	$10.0 \pm 1.2^{a,1}$	$12.0 \pm 1.1^{a,2}$	$10.7 \pm 0.4^{a,1}$	$10.5 \pm 0.6^{a,1}$	$11.6 \pm 0.8^{a,2}$	$11.1 \pm 1.4^{a,1}$	$17.2 \pm 5.7^{b,1}$	$24.6 \pm 3.0^{c,1}$
I(4)	**CONTROL**	$25.0 \pm 3.6^{a,1}$	$27.0 \pm 1.1^{a,1}$	$30.5 \pm 2.3^{a,1}$	$37.9 \pm 0.9^{b,1}$	$46.1 \pm 1.3^{c,1}$	$56.4 \pm 1.9^{d,1}$	$44.2 \pm 10.9^{bc,1}$	$51.6 \pm 7.5^{cd,1}$
	OSA	$26.4 \pm 1.6^{a,1}$	$34.0 \pm 3.7^{ab,2}$	$34.5 \pm 1.1^{b,2}$	$39.0 \pm 0.4^{bc,1}$	$45.7 \pm 0.8^{cd,1}$	$51.9 \pm 4.8^{d,1}$	$44.3 \pm 12.0^{cd,1}$	$48.1 \pm 6.6^{d,1}$
T2(5)	**CONTROL**	$25.4 \pm 2.1^{a,1}$	$23.8 \pm 0.4^{a,1}$	$24.1 \pm 0.9^{a,1}$	$28.6 \pm 2.4^{a,1}$	$50.7 \pm 8.6^{b,1}$	$62.8 \pm 13.5^{b,1}$	$97.7 \pm 23.4^{c,1}$	$103.4 \pm 32.8^{c,1}$
	OSA	$24.7 \pm 1.7^{a,1}$	$29.0 \pm 3.6^{a,2}$	$26.9 \pm 0.9^{a,2}$	$32.5 \pm 2.6^{a,1}$	$99.8 \pm 47.6^{bc,1}$	$81.2 \pm 19.4^{b,1}$	$96.7 \pm 28.4^{bc,1}$	$114.9 \pm 8.7^{c,1}$
I(5)	**CONTROL**	$24.6 \pm 4.6^{d,1}$	$24.4 \pm 2.1^{cd,1}$	$21.3 \pm 1.7^{c,1}$	$13.6 \pm 2.0^{b,1}$	$4.0 \pm 1.4^{a,1}$	$3.1 \pm 0.2^{a,1}$	$2.6 \pm 0.3^{a,1}$	$3.1 \pm 0.5^{a,1}$
	OSA	$22.9 \pm 3.5^{d,1}$	$12.9 \pm 5.1^{bc,2}$	$14.4 \pm 0.9^{c,2}$	$9.6 \pm 2.4^{b,2}$	$2.4 \pm 1.0^{a,1}$	$2.6 \pm 0.3^{a,1}$	$3.0 \pm 0.5^{a,1}$	$4.3 \pm 3.9^{a,1}$

Mean value ± standard deviation. Values followed by the same letter in the row are not significantly different ($p > 0.05$). Values followed by the same number in the column within the same parameter are not significantly different ($p > 0.05$)

After heating at 90 °C and cooling back at 20 °C, the intensity of the FID signal (I(1) + I(2)) decreased significantly for OSA dough (Table 1) compared to the same sample before heating; meanwhile, the intensity of the CPMG signal (I(3) + I(4) + I(5)) increased. On the contrary, very few changes were observed for the FID and CPMG relative intensities of CONTROL dough before and after heating and cooling. Lower solid intensity suggested that the gel cooling combined with early starch retrogradation was lower for OSA dough. At the same time, OSA dough displayed significantly shorter T2 values after a heating-cooling cycle (Table 1).

Changes in Mechanical Properties of Dough

The results of the creep curve analysis for creep and recovery phases showed that although there was a considerable variation in the values of creep test parameters between the two dough systems (CONTROL and OSA), the major features of the creep behaviour with increasing temperature was similar (Table 3, Fig. 2), with three marked domains.

Temperature-Associated Changes

Domain 1. The temperature increase up to 40 °C caused a decrease in dough resistance to deformation as shown by the increase in the maximum creep compliance, J_{max} ($p < 0.05$, Table 3, Fig. 2a). Likewise, a decrease in zero shear viscosity (Table 3, Fig. 2b) was observed ($p > 0.05$), being the lowest at 40 °C regardless of the dough system (CONTROL or OSA). This is explained by protein macromolecules unfolding which increases the dough flow ability (Domenek et al. 2002; Cristina M. Rosell and Foegeding 2007; Hayta and Schofield 2004). The maximum value of J_{max} at 40 °C could be attributed to a decrease in elasticity strength. This has been attributed to the increase in gluten mobility within the temperature range of 20–50 °C as previously demonstrated by dynamic thermomechanical analysis (on the basis of the elastic modulus) (Lefebvre et al. 2000; Rouillé et al. 2010). The authors indicated, indeed, that temperature increase up to 40 °C affected gluten chain mobility and possibly H bonds, but not the chemical structure of the gluten network. Starch granules also reversibly swelled in this temperature range, which was accompanied by polymer leaching (mainly amylose), as recently demonstrated using NMR (Rondeau-Mouro et al. 2015). The increase in temperature up to 40 °C caused the decrease in elastic recovery (J_e/J_{max} in Table 3, Fig. 2c) ($p > 0.05$).

Domain 2. Further temperature increase up to 70 °C caused the decrease of J_{max} values, indicating the increase in dough resistance to deformation (Table 3, Fig. 2a). Moreover, the lower values of J_e/J_{max} within this domain for CONTROL dough in relation to domain 1 (Table 3,

Table 3 Parameters of creep and recovery analysis of CONTROL and OSA dough during heating

		20 °C	30 °C	40 °C	50 °C	60 °C	65 °C	70 °C	73 °C	76 °C	80 °C	90 °C
Creep phase												
J_{max}, 10^{-5} Pa^{-1}	**CONT**	$98.90 \pm 0.26^{a,1}$	$152.14 \pm 1.01^{b,1}$	$180.71 \pm 7.07^{c,1}$	$144.64 \pm 17.69^{b,1}$	$18.34 \pm 1.34^{d,1}$	$10.07 \pm 0.18^{de,1}$	$2.76 \pm 0.03^{de,1}$	$2.75 \pm 0.17^{e,1}$	$2.73 \pm 0.13^{e,1}$	$2.71 \pm 0.12^{e,1}$	$3.97 \pm 0.07^{e,1}$
	OSA	$60.82 \pm 0.41^{a,2}$	$86.38 \pm 9.30^{b,2}$	$99.74 \pm 3.84^{c,2}$	$80.28 \pm 10.33^{b,2}$	$11.72 \pm 1.51^{d,2}$	$7.52 \pm 0.21^{d,2}$	$2.19 \pm 0.03^{d,2}$	$2.58 \pm 0.11^{d,1}$	$2.51 \pm 0.10^{d,1}$	$2.70 \pm 0.15^{d,1}$	$4.51 \pm 0.09^{d,2}$
h_0, 10^5 Pas	**CONT**	$4.26 \pm 0.28^{a,1}$	$3.10 \pm 0.04^{a,1}$	$2.17 \pm 0.15^{a,1}$	$2.72 \pm 0.12^{a,1}$	$19.92 \pm 1.92^{b,1}$	$42.34 \pm 1.15^{c,1}$	$142.25 \pm 4.88^{d,1}$	$168.30 \pm 1.50^{e,1}$	$193.25 \pm 1.55^{f,1}$	$207.70 \pm 15.98^{g,1}$	$162.85 \pm 4.45^{e,1}$
	OSA	$7.38 \pm 0.21^{a,2}$	$5.69 \pm 0.35^{a,2}$	$4.26 \pm 0.07^{a,2}$	$5.34 \pm 0.50^{a,2}$	$31.48 \pm 5.73^{b,2}$	$71.24 \pm 1.12^{c,2}$	$149.13 \pm 8.42^{d,1}$	$172.14 \pm 1.02^{e,1}$	$197.64 \pm 1.17^{fg,1}$	$217.90 \pm 4.19^{dg,1}$	$178.50 \pm 17.96^{ef,1}$
Recovery phase												
Je/Jmax, %	**CONT**	$69.74 \pm 0.73^{ab,1}$	$66.91 \pm 1.02^{abc,1}$	$63.17 \pm 2.42^{acd,1}$	$59.28 \pm 2.28^{cde,1}$	$59.39 \pm 2.63^{cde,1}$	$57.45 \pm 1.05^{de,1}$	$53.44 \pm 7.07^{e,1}$	$62.94 \pm 1.05^{acd,1}$	$71.76 \pm 1.14^{b,1}$	$81.57 \pm 7.37^{f,1}$	$89.95 \pm 5.86^{f,1}$
	OSA	$71.57 \pm 0.74^{ab,1}$	$69.82 \pm 2.00^{ab,1}$	$66.13 \pm 0.72^{acd,1}$	$62.35 \pm 0.84^{c,1}$	$63.32 \pm 2.15^{cd,1}$	$69.21 \pm 0.86^{abd,2}$	$72.81 \pm 2.91^{b,1}$	$83.25 \pm 1.14^{e,2}$	$86.45 \pm 1.24^{ef,2}$	$88.68 \pm 4.63^{ef,1}$	$94.25 \pm 2.63^{g,2}$
Jv/Jmax, %	**CONT**	$30.26 \pm 0.73^{ab,1}$	$33.09 \pm 1.02^{abc,1}$	$36.83 \pm 2.42^{acd,1}$	$40.72 \pm 2.28^{cde,1}$	$40.61 \pm 2.63^{cde,1}$	$42.55 \pm 1.05^{de,1}$	$46.56 \pm 7.07^{e,1}$	$37.06 \pm 1.05^{acd,1}$	$28.24 \pm 1.14^{b,1}$	$18.43 \pm 7.37^{f,1}$	$10.05 \pm 5.86^{f,1}$
	OSA	$28.43 \pm 0.74^{ab,1}$	$30.18 \pm 2.00^{ab,1}$	$33.87 \pm 0.72^{acd,1}$	$37.65 \pm 0.84^{c,1}$	$36.68 \pm 2.15^{cd,1}$	$30.79 \pm 0.86^{abd,2}$	$27.19 \pm 2.91^{b,1}$	$16.76 \pm 1.14^{e,2}$	$13.56 \pm 1.24^{ef,2}$	$11.32 \pm 4.63^{ef,1}$	$5.75 \pm 2.63^{g,2}$

Mean value ± standard deviation. Values followed by the same letter in the row are not significantly different ($p > 0.05$). Values followed by the same number in the column are not significantly different ($p > 0.05$)

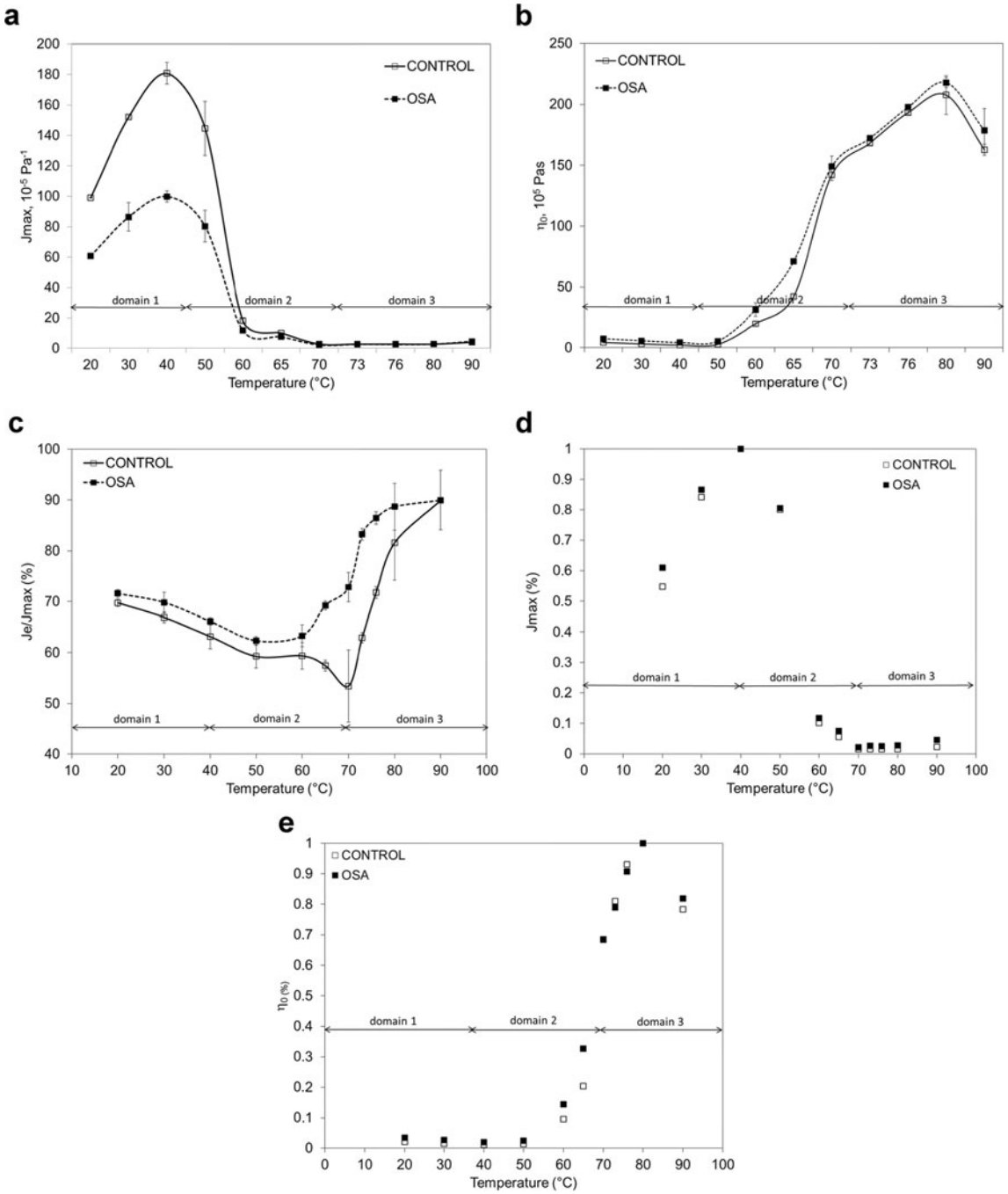

Fig. 2 Changes in maximum creep compliance (Jmax) (**a**), zero shear viscosity (η0) (**b**) and the relative elastic portion (Je/Jmax) of CONTROL and OSA dough during heating; all data from the analysis of creep and recovery tests are reported in Table 3. Relative change of Jmax (**d**) and (η0) (**e**) within the applied temperature range. Mean and standard deviation of 3 runs

Fig. 2c) was observed indicating lower portion of elastic component. The same was true for OSA dough but up to 65 °C, a point which will be further discussed in "About the Differences Between OSA and CONTROL". The effects of heat treatment on dough rheology in this period arose from two phenomena taking place at the molecular level: conformational changes of gluten proteins and starch gelatinization (melting of crystallites accompanied by water sorption), both affected by the water availability. The conformational changes within the gluten matrix comprised of gliadin and glutenin unfolding, resulting in the exposition of hydrophobic protein zones which ultimately stimulate new hydrophobic interactions, the reorganization of disulfide bonds and finally protein aggregation (Domenek et al. 2002). Consequently, an increase in the dough rigidity in this phase of processing

was observed. Simultaneously, water, including that released by gluten, was uptaken by starch granules which improved their swelling and an increase in the value of zero shear viscosity as demonstrated in Table 3 and Fig. 2b (Dreese et al. 1988); this increase persisted up slightly beyond domain 2 (up to 80 °C).

At the end of domain 2 (70 °C), both systems expressed the lowest J_{max} values (Table 3, Fig. 2a) due to the maximum of starch gelatinization (equilibrium point between granule swelling and polymer leaching), which in water limited system (such as dough) occurred in the temperature range 60–70 °C, as indicated by DSC measurements (Rouillé et al. 2010). In this temperature range, the starch granules are tightly packed and occupy larger volume than that at other temperatures due to maximum swelling, so the system expressed the highest rigidity and consequently the lowest J_{max} value.

Domain 3. Temperature increase from 70 to 90 °C affected the slight increase in J_{max} ($p > 0.05$), indicating the reduction of dough resistance due to the continuous gelatinization effects causing more destruction of residual swollen starch granules with temperature and water availability. Moreover, the elasticity of dough in this period, as evaluated by J_e/J_{max} values, increased in relation to previous period for both systems, indicating the formation of an elastic crumb. Simultaneously, zero shear viscosity decreased above 80 °C, being in accordance with the results of Dreese et al. (1988) who reported the increase in elastic modulus (*G'*) and .decrease in *tan δ* caused by heating of gluten-starch-water doughs up to 90 °C.

About the Differences Between OSA and Control

At ambient temperature, OSA dough was less extensible (lower J_{max} value) with slightly lower flowability (higher η_0 value for OSA) than CONTROL dough. Note that the same amount of total water (present as residual moisture in dry ingredients, plus that added specifically during the mixing step) was available for CONTROL and for OSA samples. Since OSA starches, as demonstrated by NMR experiment, absorb more water within the range of 20 to 50 °C (Fig. 1b), because of disrupted crystallinity after modification (Bhosale and Singhal 2007), it can be expected that less water was available for gluten, which therefore expressed higher dough rigidity resulting in less extensible dough.

All differences in dough resistance between OSA and CONTROL doughs observed in the temperature range of 20–60 °C can be related to the differences at ambient temperature since the J_{max} curves normalised by its value at 25 °C superimposed almost perfectly (Fig. 2d).

In the temperature range of starch gelatinisation and protein denaturation (60–80 °C), OSA samples were more elastic (J_e/J_{max}, Table 3, Fig. 2c) and more viscous than CONTROL ones (although they express the same relative change of resistance to deformation/zero shear viscosity with temperature (Fig. 2d, e). Indeed, OSA starch expressed higher pasting capacity, which is characteristic of both amylopectin and octenyl succinate modifications (Gupta et al. 2009; Bhosale and Singhal 2007). Another contribution could come from gluten (up to 1 %) added to the OSA dough in order to respect the starch/gluten ratio between the two recipes. Namely, gluten of higher quality is known to affect dough elasticity, but also viscosity depending on its water absorption capacity. Higher gelatinization temperature (69.7 °C instead of 63.1 °C for base flour observed by DSC for OSA starch, as mentioned above) was attributed to a higher proportion of amylopectins. However, rheological measurements did not detect this difference.

Surprisingly, OSA and CONTROL doughs behaved similarly at 80 °C but, at the end of baking (90 °C), OSA dough was more extensible (higher J_{max}) and of higher elasticity ($p < 0.05$) in comparison to CONTROL (Table 3).

Changes in Local Gas Fraction and Total Volume of Dough

Temperature-Associated Changes

Three periods could be distinguished as highlighted by MRI images in Fig. 3a and further quantified in Fig. 3b–d: (1) the first period of global expansion (0–3 min about, Fig. 3b), in the vertical direction only (Fig. 3d) consistently with pan baking, (2) the second period of decrease in section, preferentially in the vertical direction (from 3 to about 8 min, Fig. 3c, d) and (3) the third period (above 8 min) of decrease in section, preferentially in the horizontal direction—bread width (Fig. 3c, d). Characteristics of these three periods are discussed in the followings, together with the contributions from the different regions in the dough to these overall changes (Fig. 4).

Period 1. In conventional baking, the peripheral layer is the first region to be heated (Fig. 5) and to release gases, resulting in bubble growth. It hence contributed to about 80–90 % of the overall expansion (Fig. 4a). Over this short period, the peripheral layer exhibiting inflation remained thin (1.0–1.5 cm) and maximal inflation was low, 15–20 % (Fig. 3b) compared to those reported in earlier studies in the literature, about 30 %.

Periods 2–3. The decrease in dough section was severe since the section of the bread loaf after 25 min of baking was nearly the same as that of the dough before baking (Fig. 3b). Relative decrease of lower amplitude (5–30 %) was rather reported in the literature, e.g. (Sommier et al. 2005; Zanoni and Peri 1993) for bread; likewise, the decrease in volume or height during baking is little documented. These two statements justified further discussion as follows. Despite zero net inflation, the shape of the final bread section has

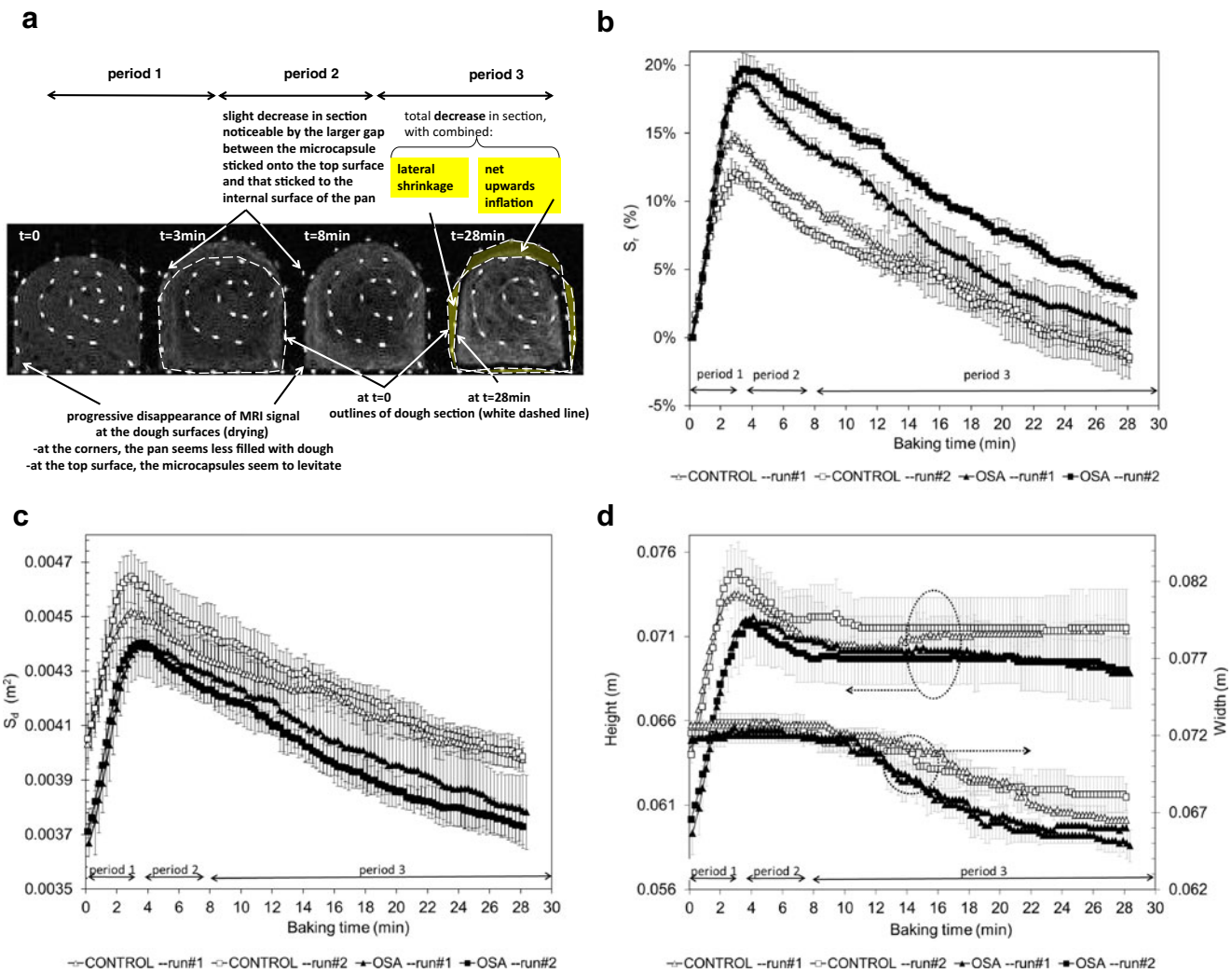

Fig. 3 Absolute and relative changes in dough section (**c**, **b**) as measured from MRI images (**a**), together with the changes in total height and width of this dough section (**d**); comparison between CONTROL and OSA. Mean and standard deviation are calculated between three MRI slices separated by 4 cm; the experiment was repeated twice. Refer to the text for further details about periods 1–3. Part of the MRI signal on images (**a**) disappeared because of dehydration (from 8 min of baking, while water content in the crust was 15 % wb); at low water contents, no signal can be acquired with the MRI protocol used. This explanation was confirmed by the "levitation" at fixed coordinates of microcapsules placed onto the top surface of the dough. In no way, this signal disappearance should be interpreted as shrinkage

changed; it was higher and less large than the section of the original dough section (Fig. 3a, d). Dough core was heated and hence inflated during period 2 mainly, implying that the area occupied by the peripheral layer of dough decreased to an even higher extent than that observed globally (Fig. 4a). The mechanisms possibly involved in the decrease in gas fraction locally or globally are:

(i) Collapse

Collapse results from insufficient gas retention and pressure combined to a rigidity of the overall structure whose mechanical properties become insufficient to counterbalance the gravity forces; consequently, the associated displacement is vertical. In the case of bread, collapse is likely to occur in the bottom region (Fig. 4b), where gravitational forces are the highest and pores are already opened and communicate with the outside (at atmospheric pressure). Externally, it is revealed by the accentuation of bumps at the bread surface the closest to the edges of the pan (Cauvain and Young 2001). It was shown by simulation of the baking process (unpublished work) that any event promoting dough rigidity, locally (e.g. later opening of the pores) or globally (e.g. formation of a thick, continuous crust) will slow down collapse. This feature will be of particular interest for the analysis of results between OSA and CONTROL systems in the next section.

(ii) Shrinkage

Little attention has been paid to shrinkage in past scientific studies. It results from the loss of water, and

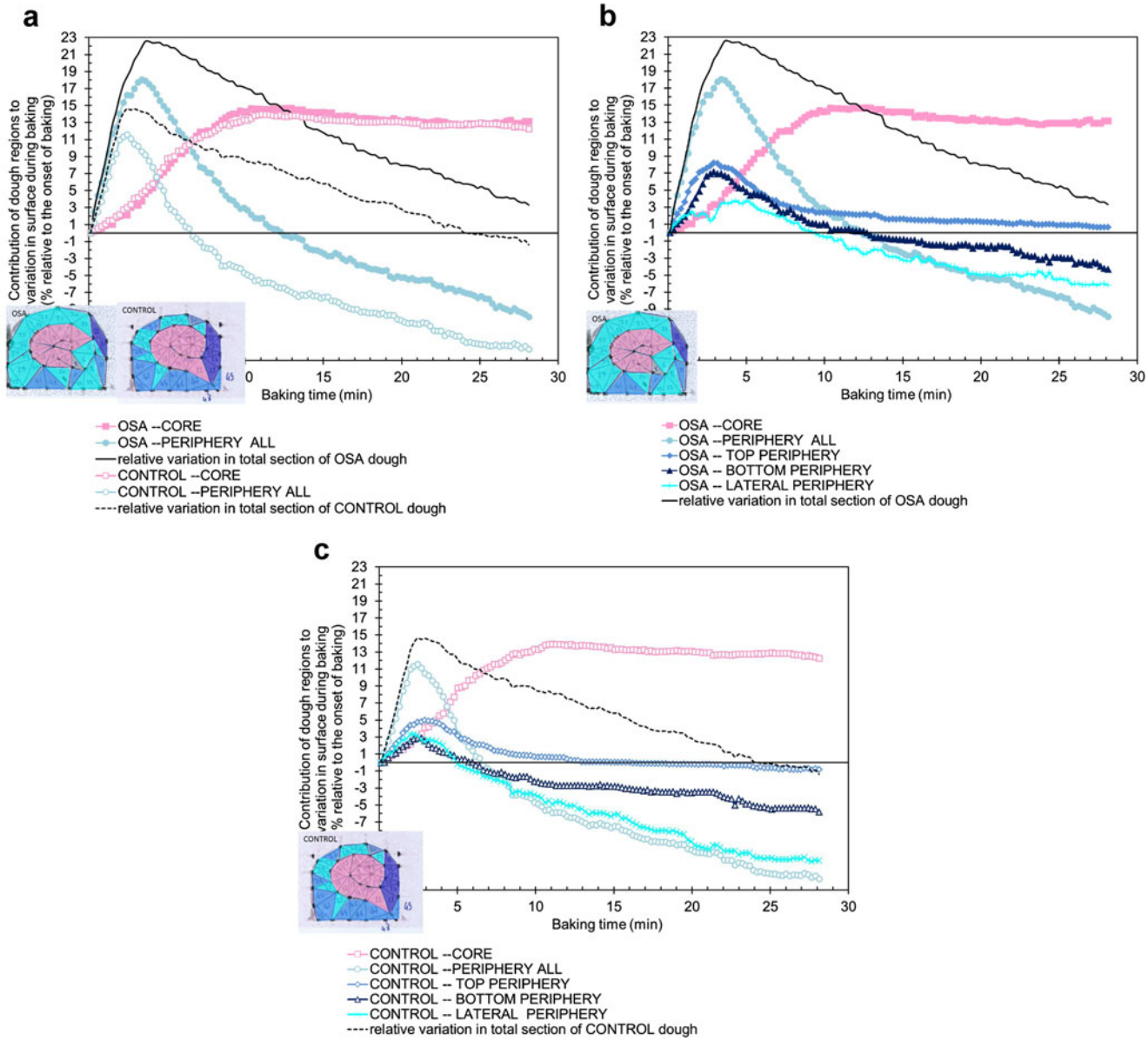

Fig. 4 Contribution of dough regions to the relative changes in total dough section during baking; comparison between OSA and CONTROL dough. **a** How the peripheral layer and the core contribute to the overall changes in dough section. **b**,**c** How the top, bottom and sides contribute to the changes in the peripheral layer, for OSA dough and CONTROL dough respectively

possibly the changes in the molecular conformation of macromolecules, e.g. protein reticulation. Cumulated over the whole perimeter of the dough section, it behaves like a belt, restricting expansion and even reducing the dough section. The extent of shrinkage observed during the drying of dough slabs (sampled just after mixing and relaxed after lamination) could explain most of the observed decrease in dough section: converting the unidirectional shrinkage estimated at about 13 % at 25 min of baking (Fig. 6) in the two dimensions of the genuine bread section yields a value of about 16 %, close to the variation in section observed between the end of period 1 and period 3 (Fig. 3b).

(iii) Squeezing

Squeezing results from the inflation at core at a rate higher than the surroundings (crust) can deform. This may explain decrease in gas fraction observed locally. Already stiffened regions will be more resistant to squeezing, the level of stiffening yet depending on their level of temperature and/or water content (Wagner et al. 2008a).

These mechanisms may take place simultaneously. It is attempted nevertheless to point out any predominant mechanism for each period of baking.

Squeezing was over once inflation has stopped throughout the dough section, at baking times higher

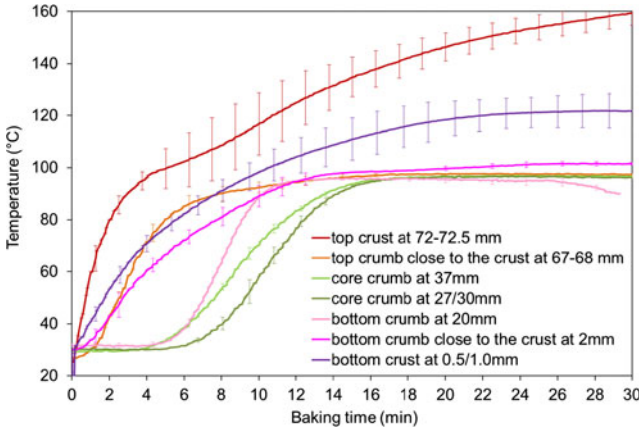

Fig. 5 Temperature at different locations in dough during MRI baking. Positions of optical fibers refer to the end of baking, motion of a few millimetres cannot be excluded during baking. They are relative to the bottom of the bread loaf, with a final total height of 73 mm in average. Mean and standard deviation of four to five runs for crust locations and two runs for crumb locations

than 11–12 min (Fig. 4a). Since the decrease in area in the top peripheral layer also ceased at that time, squeezing should be predominant at this place. It is more difficult to disentangle the mechanisms involved in the peripheral layer at the bottom. It has been recently shown by simulation with a numerical model of baking (unpublished work) that the effect of squeezing on gas fraction at the bottom of bread loaf was dominant upon collapse (factor of 4). This may explain why the rate of decrease in area of the peripheral layer during period 2 little differed between the top and bottom (Fig. 4b, c). Collapse was considered to be terminated once the total height of the loaf was relatively stable, a point which was reached at about 8 min of baking (Fig. 3d). Hence, all variations in gas fraction or dimensions at baking times higher than 11–12 min are likely to be assigned to shrinkage of the porous structure; this refers to period 3 as defined in Fig. 3.

As expected, shrinkage affected the gas fraction in the peripheral layer mainly and in the core to a much lower extent (see Fig. 4a: between 12 and 22 min of baking, the shift was of 4–6 versus 1–2 %). As the drying process in pan baking, shrinkage was also not uniform, starting at the top surface, and propagating along the sides down to the bottom (bread width decreased later, after 9–11 min of baking, Fig. 3c). Dough slabs (mimicking the dough layer present at the surface of the loaf) shrunk predominantly at the onset of water loss (from the initial water content down to 35–25 % in water content) and proceeded more slowly beyond this point (Fig. 6). Note that 25 % in the water content was attained in the top crust within 3.5 min of baking (Fig. 7), hence corresponding to the end of period 1. Shrinkage at the top impacted local gas fraction in combination and with a antagonistic effect to inflation (period 1) and further squeezing (period 2). Consistently with results on dough slabs, the rate of decrease in gas fraction at the top was much lower during period 3 where gas fraction was almost constant (Fig. 4b, c). During this period, shrinkage was higher in the bottom and in the lateral peripheral layer than in the top due to the sequential drying at the dough surface as already pointed out.

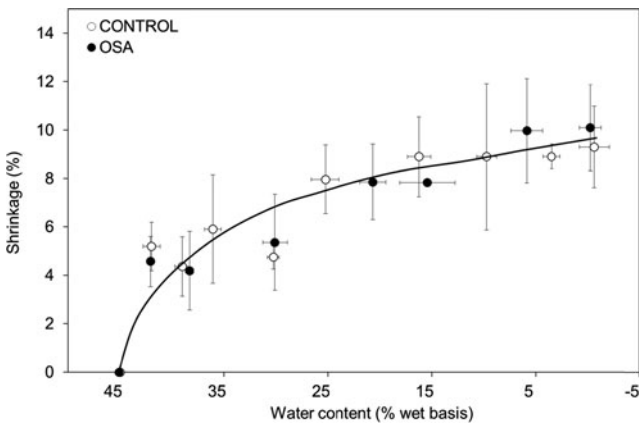

Fig. 6 Shrinkage (expressed in % relative to the initial surface) of CONTROL and OSA dough slabs, laminated just after mixing (4–5 mm) and relaxed for 10 min before drying. Mean and standard deviation of more than 7 runs, with 4 replicates each. Temperature during drying was consistent with that at the surfaces of bread dough during baking (Fig. 5)

About the Differences Between OSA and Control

The section of OSA dough was lower at the end of proving (about 9 %, Fig. 3c). Note that this observation would not have been noticed without the use of a non-invasive technique. This difference in volumes was surprising since a reference dough piece for volume checking was used during

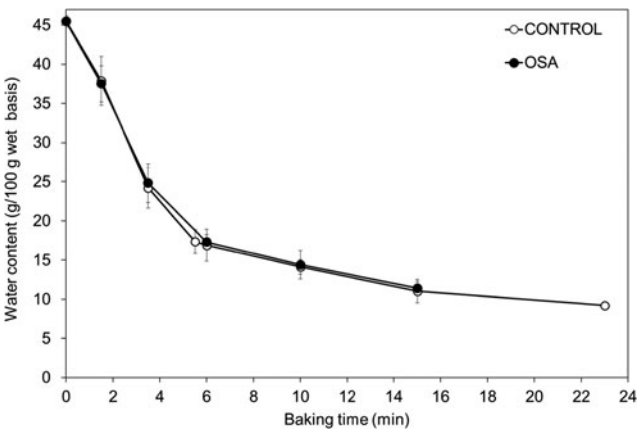

Fig. 7 Water content in the top crust during baking; effect of OSA starch used in the dough preparation. Mean and standard deviation of 3 runs

proving (see section "Materials and Methods"). At the contrary to the dough piece, the dough to be baked was shaped. As OSA dough was more elastic (Table 3), the residual strains after the shaping step could still be noticeable after 45 min of proving, with an impact on the volume. This difference explained why relative section (Fig. 3b) mainly served for further analysis during baking. This analysis is carried out chronologically.

Rate of inflation was the same during the first period of baking (period 1 as defined above), no matter the dough system. This did not reflect the higher resistance of OSA dough to deformation (Table 3); likewise, modelling studies of baking showed that inflation could be explained by viscosity alone (unpublished work) and only slightly higher flowability was observed for OSA dough (Table 3, with the temperature range for period 1 displayed in Fig. 5 and equal to 30–50 °C at the exception of the first millimetres).

Maximal inflation (end of period 1) was higher for OSA dough (+6 %, Fig. 3b). Since the inflation rate was the same, this meant that maximal expansion was reached at a slightly longer time of baking for OSA dough (3.6 vs. 2.8 min). Different explanations can be proposed for this. An impact of the resistance to deformation is not plausible since the dough inflated at the same rate in the two dough systems (Fig. 3b). A higher resistance of dough to rupture at the dough wall scale could provide a longer retention of gases. Although this property was not assessed, it is often positively correlated to elasticity, and a higher elasticity was reported for OSA dough (Table 3). A last possible explanation was a delayed process of collapse. During period 2, the rate of decrease in dough section (Fig. 3b) and especially in height (Fig. 3d) was slightly lower for OSA dough. Likewise, the bottom region in OSA dough exhibited a later decrease in area than in CONTROL dough (compare between Fig. 4b, c). Indeed, during this timeframe (3–8 min of baking), the bottom region (of 15 mm thick) presented a lower flowability for OSA (Table 3) with its temperature passing over the temperature range of 50–70 °C (Fig. 5). As a preliminary conclusion, at the end of period 2, the addition of OSA starch increased the baking performance of the flour selected for this study.

During period 3, the section of OSA loaves decreased at a higher rate than for CONTROL loaves, resulting in an even baking performance between the two dough systems at the end of period 3 (Fig. 3b). On the one hand, the ability to shrink subsequently to dehydration did not reveal to be different between dough systems (Fig. 6), although differences might have been hidden by the large variability of results. On the other hand, higher density in the peripheral dough layer where the vaporization front progresses is known to accelerate dehydration; these higher levels of density could be expected in OSA dough because of a lower volume at the beginning of baking. The contribution of shrinkage to densification in the peripheral dough layer was significant compared to that of squeezing that took place during period 2 (when the core expanded while the crust has lost its capacity to deform): ¼ for CONTROL (−7 out of −25 %, with reference to the maximal inflation achieved in period 1) and 1/3 for OSA (−11 out of −28 %, with reference to the maximal inflation achieved in period 1).

At the end of baking (25 min), the section of OSA bread loaves was lower: by about 5 % when prepared for MRI measurements (Fig. 3b) and 12 % based on measurements with millet seed displacement on loaves baked in a conventional oven (3.13 ± 0.15 vs. 3.55 ± 0.08 m^3/kg, $p < 0.05$). This was mainly explained by the lower initial volume of OSA dough (9 % in the MRI baking condition) and partly counterbalanced by the higher baking performance of OSA dough noticed during periods 1 and 2 (yielding a lower volume by 5 % only at the end of baking).

Characterization of Final Bread Quality

The impact of OSA starch incorporation on final bread quality (colour and texture) is summarized in Table 4.

The Differences in Colour Between OSA and Control

In general, OSA dough yielded bread with lighter crust and lower browning index in comparison to the CONTROL bread ($p < 0.05$), wherein the total colour difference in crust colour was considered obvious for the human eye (Francis and Clydesdale 1975). The observed effect was explained by the reduced susceptibility of OSA starch to enzymatic

Table 4 Colour and TPA results obtained on final bread loaves; comparison between OSA and CONTROL bread loaves

	CONTROL	OSA
Crust colour		
Lightness (L*)	68.66 ± 3.49^a	72.90 ± 3.86^b
Browning index	86.06 ± 14.15^a	54.86 ± 16.02^b
Total colour difference	–	70.71
Crumb colour		
Lightness (L*)	68.92 ± 0.42^a	68.61 ± 1.31^a
Whiteness index	63.74 ± 0.45^a	63.75 ± 1.20^a
Total colour difference	–	0.65
TPA		
Hardness, g	10485 ± 1178^a	14467 ± 921^b
Springiness	0.98 ± 0.01^a	0.97 ± 0.01^a
Cohesiveness	0.77 ± 0.01^a	0.78 ± 0.01^a
Chewiness, g	7948 ± 896^a	10884 ± 665^b
Resilience	0.40 ± 0.01^a	0.43 ± 0.01^b

Mean value ± standard deviation. Values followed by the same letter in the row within the same parameter are not significantly different ($p > 0.05$)

degradations (α-amylase, amyloglucosidase and pullulanase) caused by the presence of octenyl succinate groups in the starch chains (Viswanathan 1999). Therefore, the formation of melanoidins as products of Maillard reaction, which are responsible for bread browning during baking, occurred to a smaller extent in OSA bread formulation. Schmidl (1983) demonstrated that the use of OSA modified starch in combination with a mono- and diglycerides emulsifier provided acceptable emulsification stability, while reducing the Maillard reaction. Considering the crumb colour, no difference between CONTROL and OSA sample was observed ($p > 0.05$), with the total colour differences not obvious for the human eye.

The Differences in Crumb Textural Properties Between OSA and Control

The presence of OSA starch in bread formulation increased the hardness and chewiness of bread crumb ($p < 0.05$) in comparison to CONTROL bread, being in accordance with the results of specific bread volume due to the fact that hardness, as a bread crumb feature, is largely influenced by the volume and density of bread loaves (Skendi et al. 2010; Hadnađev et al. 2014; Goesaert et al. 2008) This was also a consequence of higher rigidity of OSA dough in relation to CONTROL (lower values of J_{max}, Table 3); Lazaridou et al. (2007) also showed that the higher rigidity of dough results in breads with low loaf volumes and high crumb hardness. In fact, such rheological behaviour of OSA dough might have affected the thickening of the crumb walls surrounding gas bubbles which was reflected in increased hardness of OSA bread crumb (C. M. Rosell et al. 2001). Dough prepared with OSA starch also displayed shorter NMR T2 values after heating and cooling at 20 °C (Table 1) may be due to a lower proton mobility in this sample, in relation with the bread crumb hardness (Bosmans et al. 2014; Curti et al. 2014) (Table 3). Furthermore, springiness, which refers to the crumb elasticity (Bourne 2002), and cohesiveness were not significantly affected by the presence of OSA starch in formulation. Conversely, resilience of OSA breads which represents "instantaneous springiness", slightly decreased ($p < 0.05$) in comparison to CONTROL.

Discussion

Different methods for dough investigation used in the present study provided a means of linking the phenomena occurring at multiple scales during baking. The analysis was refined by comparing the results obtained on two bread formulations.

A higher absorption of water by OSA starch granules was evidenced by NMR. This difference, significant at 30 and 40 °C, persisted up to 60 °C. It can explain the higher rigidity of OSA dough over this temperature range (J_{max} in creep recovery tests was double for OSA compared to CONTROL dough). The value of the longest transverse relaxation time measured by NMR did not differ between CONTROL and OSA doughs in this temperature range, showing that the water phase of the two systems is close in composition and physicochemical properties below the gelatinization onset.

Turning to the temperature range of starch gelatinisation, the higher proportion of amylopectin and OSA modifications in OSA starch expressed in a higher pasting capacity of OSA dough, higher rigidity and slightly higher viscosity. Still, in this temperature range, the shift of melting of amylopectins to higher temperatures was evidenced by a higher intensity of the NMR solid component (1) for OSA dough. Characteristic T2 values of amorphous starch protons tended to be longer in OSA dough too. This evolution in T2 values was already discussed by Rondeau-Mouro et al (2015). OSA dough seems to show higher amylose and/or gluten mobility supposed to originate from weaker inter- and/or intra-macromolecular interactions may be due to the higher water sorption capacity of OSA starch. Given the small fraction of OSA starch added to the flour, this shift was small and did not affect the longer NMR T2 components, neither the rheological behaviour of OSA dough.

Among all these differences, those observed at low temperatures (before starch gelatinisation) were the more prone to explain an extended oven-rise observed by MRI for OSA dough. In others words, differences observed between dough systems in the temperature range at which major changes in molecular structure occur (60–80 °C) were of no use for interpreting differences in oven-rise observed in this study; this might be due to the undesirable decrease in volume observed during the second step of baking and such conclusion would require confirmation with other types of flour—with a better capacity of holding of their maximal volume achieved during baking. Maximal inflation was higher (+6 %) when OSA starch was added to the flour (together with gluten so to maintain the gluten/starch ratio between the original and modified flours). This was explained by a delayed collapse of cell walls in the bottom of the dough, which presented higher resistance to deformation for OSA dough in this temperature range (50–70 °C). Again, this mechanical feature was related to the higher absorption of water by OSA starch granules.

During the second step of baking (required for complete heating, resulting in the transition from dough to crumb at core and also the coloration of the crust), collapse of the porous structure combined to persistent shrinkage consecutively to water loss compensated for the volume gained during the first period of baking. Shrinkage was stronger for OSA dough yielding to an even overall baking performance between the two dough systems. The explanation for this enhanced shrinkage could not be retrieved exactly, a higher loss of water in OSA dough being the most plausible cause.

The textural properties of bread crumb were mostly a reflection of rheological properties of dough, being firmer

for OSA starch containing bread and confirmed by lower water proton mobility as measured by NMR. In the same time, NMR applied to cooled samples indicated a lower proportion of protons with constrained motions for OSA dough. This result was surprising and could be related with differences in the gel cooling and/or starch retrogradation process, which would need further investigation. The increased crumb hardness could be counterbalanced by using the amount of water optimal for the preparation of OSA dough.

Conclusion

In conclusion, the overall results showed that differences in "macroscopic" changes during baking between OSA and CONTROL dough were rather explained by the characteristics of dough before starch gelatinisation than those at temperatures 60–80 °C at which major changes in molecular structure occur. Higher absorption of water by OSA starch granules as measured by NMR yielded higher rigidity of OSA dough before the onset of starch gelatinisation and delayed collapse at the bottom of bread dough during baking. The approach used also demonstrated the interest of dynamic monitoring of the inflation during baking, allowing to target the baking period and the plausible mechanism responsible for lower specific volume. Indeed, MRI monitoring showed that the addition of OSA starch to flour improved the baking performance during the first steps of baking, but enhanced the shrinkage of the structure during the last steps of baking. Finally, mechanical properties and molecular motions were coherent and strongly linked, suggesting very different water-biopolymer interactions in OSA dough and final bread, not surprising a result if we consider the structure of OSA starch with a higher proportion of amylopectin and capacity of water sorption but rather remarkable if we consider the low content of OSA replaced in the CONTROL recipe. Future investigation should search for ways of counter-balancing low final volume default, either by further understanding the mode of action of OSA starch during shrinkage, or by combination of improvers, or different processing pathways. In order to perceive the overall potential of OSA starch as a specific bread dough ingredient, the experiment should be repeated in an identical manner with flours of different technological quality especially in terms of different qualities of protein and starch components and combinations thereof. Moreover, carrying out the experiment with optimum amount of water is also required for closer understanding the mechanisms aforementioned explained in the real systems which may contribute to the specific problems solving in the manufacture of baked products and the formulation of specialty baking products, as well.

Acknowledgments This study was supported by the PHC Curien Savic Research Program and bilateral scientific cooperation between Serbia and France. This work was partly financed by the Ministry of Education, Science and Technological Development, Republic of Serbia (TR31007). Part of this work (NMR and MRI) was realized using the facilities and resources of PRISM platform (Rennes, France). The authors thank Dominique Le Ray (IRSTEA, Rennes) for his assistance with NMR measurements and bread-making procedures.

References

Aguilera, J. M. (2005). Why food microstructure? *Journal of Food Engineering, 67*(1-2), 3–11.

Bajd, F., & Sersa, I. (2011). Continuous monitoring of dough fermentation and bread baking by magnetic resoannce microscopy. *Magnetic Resonance Imaging, 29*, 434–442.

Besbes, E., Jury, V., Monteau, J. Y., & Le Bail, A. (2013). Characterizing the cellular structure of bread crumb and crust as affected by heating rate using X-ray microtomography. *Journal of Food Engineering, 115*(3), 415–423.

Bhosale, R., & Singhal, R. (2007). Effect of octenylsuccinylation on physicochemical and functional properties of waxy maize and amaranth starches. *Carbohydrate Polymers, 68*(3), 447–456.

Bosmans, G. M., Lagrain, B., Deleu, L. J., Fierens, E., Hills, B. P., & Delcour, J. A. (2012). Assignments of proton populations in dough and bread using NMR relaxometry of starch, gluten, and flour model systems. *Journal of Agricultural and Food Chemistry, 60*(21), 5461–5470.

Bosmans, G. M., Lagrain, B., Fierens, E., & Delcour, J. A. (2013a). The impact of baking time and bread storage temperature on bread crumb properties. *Food Chemistry, 141*(4), 3301–3308.

Bosmans, G. M., Lagrain, B., Ooms, N., Fierens, E., & Delcour, J. A. (2013b). Biopolymer interactions, water dynamics, and bread crumb firming. *Journal of Agricultural and Food Chemistry, 61*(19), 4646–4654.

Bosmans, G. M., Lagrain, B., Ooms, N., Fierens, E., & Delcour, J. A. (2014). Storage of parbaked bread affects shelf life of fully baked end product: A H-1 NMR study. *Food Chemistry, 165*, 149–156.

Bourne, M. C. (2002). *Food texture and viscosity: concept and measurement*. UK: Academic Press.

Cauvain S. P., & Young, L. S. (2001). *Baking problems solved*. Cambridge, UK: Woodhead Publishing in Food Science and Technology.

Cauvain, S. P., & Young, L. S. (2009). *The ICC handbook of cereals, flour, dough and product testing: methods and applications*. Pennsylvania: DEStech Publications, Inc.

Chen, P. L., Long, Z., Ruan, R., & Labuza, T. P. (1997). Nuclear magnetic resonance studies of water mobility in bread during storage. *LWT Food Science and Technology, 30*(2), 178–183.

Chiotelli, E., Pilosio, G., & Le Meste, M. (2002). Effect of sodium chloride on the gelatinization of starch: a multi measurement study. *Biopolymers, 63*(1), 41–58.

Chung, H. J., Lee, S. E., Han, J. A., & Lim, S. T. (2010). Physical properties of dry-heated octenyl succinylated waxy corn starches and its application in fat-reduced muffin. *Journal of Cereal Science*, *52*, 496–501.

Curti, E., Bubici, S., Carini, E., Baroni, S., & Vittadini, E. (2011). Water molecular dynamics during bread staling by nuclear magnetic resonance. *LWT–Food Science and Technology, 44*(4), 854–859.

Curti, E., Carini, E., Tribuzio, G., & Vittadini, E. (2014). Bread staling: effect of gluten on physico-chemical properties and

molecular mobility. *LWT–Food Science and Technology, 59*(1), 418–425.

Dobraszczyk, B. J., & Morgenstern, M. (2003). Rheology and the breadmaking process. *Journal of Cereal Science, 38*(3), 229–245.

Domenek, S., Morel, M. H., Bonicel, J., & Guilbert, S. (2002). Polymerization kinetics of wheat gluten upon thermosetting. A mechanistic model. *Journal of Agricultural and Food Chemistry, 50*(21), 5947–5954.

Donald, A. M. (2004). Understanding starch structure and functionality. In A.-C. Eliasson (Ed.), *Starch in food: structure, function and applications* (pp. 171–199). Cambridge: Woodhead Publishing Limited.

Doona, C. J., & Baik, M. Y. (2007). Molecular mobility in model dough systems studied by time-domain nuclear magnetic resonance spectroscopy. *Journal of Cereal Science, 45*(3), 257–262.

Dokić, L. J., Krstonošić, V., & Nikolić, I. (2012). Physicochemical characteristics and stability of oil-in-water emulsions stabilized by OSA starch. *Food Hydrocolloids*, *29*, 185–192.

Dreese, P. C., Faubion, J. M., & Hoseney, R. C. (1988). Dynamic rheological properties of flour, gluten, and gluten-starch doughs. 1. Temperature-dependent changes during heating. *Cereal Chemistry, 65*(4), 348–353.

Engelsen, S. B., Jensen, M. K., Pedersen, H. T., Norgaard, L., & Munck, L. (2001). NMR-baking and multivariate prediction of instrumental texture parameters in bread. *Journal of Cereal Science, 33*(1), 59–69.

Francis, F. J., & Clydesdale, F. M. (1975). *Food colorimetry: theory and applications*. Wesport, Connecticut: The Avi publishing company, INC.

Gil, A. M. (2003). Techniques for analysing wheat proteins. In S. P. Cauvain (Ed.), *Bread making: improving quality* (pp. 97–120). Cambridge: Woodhead Publishing Limited.

Goesaert, H., Leman, P., & Delcour, J. A. (2008). Model approach to starch functionality in bread making. *Journal of Agricultural and Food Chemistry, 56*(15), 6423–6431.

Gupta, M., Bawa, A. S., & Semwal, A. D. (2009). Morphological, thermal, pasting, and rheological properties of barley starch and their blends. *International Journal of Food Properties, 12*(3), 587–604.

Hadnađev, T. R. D., Dokić, L. P., Hadnađev, M. S., Pojić, M. M., & Torbica, A. M. (2014). Rheological and breadmaking properties of wheat flours supplemented with octenyl succinic anhydride-modified waxy maize starches. *Food and Bioprocess Technology, 7*(1), 235–247.

Hayta, M., & Schofield, J. D. (2004). Heat and additive induced biochemical transitions in gluten from good and poor breadmaking quality wheats. *Journal of Cereal Science, 40*(3), 245–256.

ICC (1996). ICC standard method 110/1. *Determination of the moisture content of cereals and cereal products*. Vienna, International Association for Cereal Science and Technology.

Jenkins, P. J., & Donald, A. M. (1998). Gelatinisation of starch: a combined SAXS/WAXS/DSC and SANS study. *Carbohydrate Research, 308*(1-2), 133–147.

Kapur, J. N., Sahoo, P. K., & Wong, A. K. C. (1985). A new method for gray_level picture thresholding using the entropy of the histogram. *Computer Vision Graphics and Image Processing, 29*(3), 273–285.

Kim, G.-W., Kim, M.-S., Sagara, Y., Bae, Y.-H., Lee, I.-B., Do, G.-S., et al. (2008). Determination of the viscoelastic properties of apple flesh under quasi-static compression based on finite element method optimization. *Food Science and Technology Research, 14*(3), 221–231.

Lakes, R. (1993). Materials with structural hierarchy. *Nature, 361*(6412), 511–515.

Laridon, Y., Doursat, C., Grenier, D., Michon, C., Flick, D., & Lucas, T. (2015). Identification of broad-spectrum viscoelastic parameters: influence of experimental bias on their accuracy and application to semihard-type cheese. *Journal of Rheology, 59*(4), 1019–1044.

Lazaridou, A., Duta, D., Papageorgiou, M., Belc, N., & Biliaderis, C. G. (2007). Effects of hydrocolloids on dough rheology and bread quality parameters in gluten-free formulations. *Journal of Food Engineering, 79*(3), 1033–1047.

Lefebvre, J., Popineau, Y., Deshayes, G., & Lavenant, L. (2000). Temperature-induced changes in the dynamic rheological behavior and size distribution of polymeric proteins for glutens from wheat near-isogenic lines differing in HMW glutenin subunit composition. *Cereal Chemistry, 77*(2), 193–201.

Lucas, T., Wagner, M., Quellec, S., & Davenel, A. (2008). NMR imaging of bread and biscuit. In G. A. Webb (Ed.), *Modern magnetic resonance, Part 3: applications in materials science and foodscience* (pp. 1795–1799). Dordercht: Springer.

Mirsaeedghazi, H., Emam-Djomeh, Z., & Mousavi, S. M. A. (2008). Rheometric measurement of dough rheological characteristics and factors affecting it. *International Journal of Agriculture and Biology, 10*, 112–119.

Mondal, A., & Datta, A. K. (2008). Bread baking—a review. *Journal of Food Engineering, 86*(4), 465–474.

Reiner, S. J., Reineccius, G. A., & Peppard, T. L. (2010). A comparison of the stability of beverage cloud emulsions formulated with different gum acacia- and starch-based emulsifiers. *Journal of Food Science*, *75*(5), E236–E246.

Rondeau-Mouro, C., Cambert, M., Kovlrija, R., Musse, M., Lucas, T., & Mariette, F. (2015). Temperature-associated proton dynamics in wheat starch-based model systems and wheat flour dough evaluated by NMR. *Food and Bioprocess Technology, 8*(4), 777–790.

Rosell, C. M., & Foegeding, A. (2007). Interaction of hydroxypropylmethylcellulose with gluten proteins: small deformation properties during thermal treatment. *Food Hydrocolloids, 21*(7), 1092–1100.

Rosell, C. M., Rojas, J. A., & de Barber, C. B. (2001). Influence of hydrocolloids on dough rheology and bread quality. *Food Hydrocolloids, 15*(1), 75–81.

Rouillé, J., Chiron, H., Colonna, P., Della Valle, G., & Lourdin, D. (2010). Dough/crumb transition during French bread baking. *Journal of Cereal Science, 52*(2), 161–169.

Saricoban, C., & Yilmaz, M. T. (2010). Modelling the effects of processing factors on the changes in colour parameters of cooked meatballs using response surface methodology. *World Applied Sciences Journal, 9*, 14–22.

Schiraldi, A., & Fessas, D. (2003). The role of water in dough formation and bread quality. In S. P. Cauvain (Ed.), *Bread making: Improving quality* (pp. 306–320). Cambridge: Woodhead Publishing Limited.

Schmidl, M. K. (1983). Liquid elemental diet. US Patent No. 4,414,238.

Skendi, A., Biliaderis, C. G., Papageorgiou, M., & Izydorczyk, M. S. (2010). Effects of two barley beta-glucan isolates on wheat flour dough and bread properties. *Food Chemistry, 119*(3), 1159–1167.

Sommier, A., Chiron, H., Colonna, P., Della Valle, G., & Rouille, J. (2005). An instrumented pilot scale oven for the study of French bread baking. *Journal of Food Engineering, 69*(1), 97–106.

Turbin-Orger, A., Boller, E., Chaunier, L., Chiron, H., Della Valle, G., & Reguerre, A. L. (2012). Kinetics of bubble growth in wheat flour dough during proofing studied by computed X-ray micro-tomography. *Journal of Cereal Science, 56*(3), 676–683.

Van Duynhoven, J. P. M., Van Kempen, G. M. P., Van Sluis, R., Rieger, B., Weegels, P., Van Vliet, L. J., et al. (2003). Quantitative assessment of gas cell development during the proofing of dough by magnetic resonance imaging and image analysis. *Cereal Chemistry, 80*(4), 390–395.

Viswanathan, A. (1999). Effect of degree of substitution of octenyl succinate starch on enzymatic degradation. *Journal of Environmental Polymer Degradation, 7*(4), 185–190.

Wagner, M., Quellec, S., Trystram, G., & Lucas, T. (2008a). MRI evaluation of local expansion in bread crumb during baking. *Journal of Cereal Science, 48*(1), 213–223.

Wagner, M., Loubat, M., Sommier, A., Le Ray, D., Collewet, G., Broyart, B., et al. (2008b). MRI study of bread baking: experimental device and MRI signal analysis. *International Journal of Food Science and Technology, 43*(6), 1129–1139.

Waigh, T. A., Gidley, M. J., Komanshek, B. U., Donald, A. M. (2000). The phase transformations in starch during gelatinisation: a liquid crystalline approach. *Carbohydrate Research, 328*(2), 165–176.

Wang, X., Choi, S. G., & Kerr, W. L. (2004). Water dynamics in white bread and starch gels as affected by water and gluten content. *LWT–Food Science and Technology, 37*(3), 377–384.

Whitworth, M. B., & Alava, J. M. (2004). Non-destructive imaging of bread and cake structure during baking. In S. P. Cuvan, S. S. Salmon, & L. S. Young (Eds.), *Using cereal science and technology for the benefit of consumers. Proceedings of the 12th ICC Cereal & Bread Congress* (pp. 456–460). Harrogate: Woodhead Publishing Ltd.

Wynnejones, S., & Blanshard, J. M. V. (1986). Hydration studies of wheat-starch, amylopectin, amylose gels and bread by proton magnetic-resonance. *Carbohydrate Polymers, 6*(4), 289–306.

Zanoni, B., & Peri, C. (1993). A study of the bread-baking process. I: a phenomenological model. *Journal of Food Engineering, 19*(4), 389–398.